19th Brazilian Congress of Thermal Sciences and Engineering
November 6th–10th, 2022, Bento Gonçalves - RS - Brazil

ENC-2022-0355
SIMULATION OF THE FLOW FIELD AND FAR-FIELD NOISE OF AN UAV PROPELLER

Filipe Dutra da Silva
Juan Pablo de Lima Costa Salazar
Julio Victor Vieira Martins Chadlvski
Department of Mobility Engineering, Federal University of Santa Catarina, Joinville, SC, Brazil
filipe.dutra@teg.ufsc.br, juan.salazar@ufsc.br, julio.chadlvski@teg.ufsc.br

Abstract. *Recent advances in electric propulsion and unmanned aerial vehicle (UAV) design have drawn attention to the noise generated by propellers, owing to concerns with the increase of noise levels in urban areas and related adverse effects. In this scenario, numerical simulations can aid design towards quieter and aerodynamically efficient propellers. We propose an analysis and validation of a simulation model for predicting the flow and acoustic fields of propellers using the open-source code OpenFOAM. A two-blade UAV propeller geometry of diameter equal to 0.24 m was chosen from experiments conducted at the Hong Kong University of Science and Technology. Unsteady Reynolds Averaged Navier-Stokes simulations were conducted using the $k-\omega$ SST turbulence model for an isolated propeller configuration. The unstructured mesh is composed predominantly by tetrahedra, with the addition of layers of prismatic volumes in the vicinity of the propeller, in order to better resolve the boundary layer gradients. The acoustic field is obtained by using the Ffowcs-Williams and Hawkings analogy, implemented in the OpenFOAM open source LibAcoustics library, and tests are reported regarding the sensitivity of the results to the shape and size of the control surfaces used by the method. Results are validated through comparisons with experimental data for the thrust and torque coefficients and for the far-field noise. In general, the numerical results show good agreement with experimental data regarding the aerodynamic coefficients and tonal noise level.*

Keywords: *Propeller Noise, UAV Noise, OpenFOAM, RANS*

1. INTRODUCTION

With the recent advances and focus on the development of electric vertical take-off and landing (eVTOL) vehicles and unmanned aerial vehicles (UAVs), noise emitted by propellers is still a major concern. The design of low-noise propellers requires a balance between noise emission and aerodynamic performance, which tend to impact each other negatively when optimized separately.

Numerical approaches such as computational fluid dynamics (CFD) coupled with noise prediction methods can aid in the design of low-noise propellers. Among the available methods, Large-eddy simulation (LES) is a high-fidelity alternative that enables a more fundamental analysis of the noise generation and propagation mechanisms (Afari *et al.*, 2019; Avallone *et al.*, 2018). However, unsteady Reynolds Average Navier-Stokes (RANS) simulations (Chirico *et al.*, 2017; Hambrey, 2017; Ben Nasr *et al.*, 2017; Arnhem *et al.*, 2018; Stokkermans *et al.*, 2019; Bento *et al.*, 2020) can deliver reasonable results at reduced computational cost. Analytical, semi-empirical and reduced order methods are desirable in the design process largely because of the ability to quickly estimate the impact of design parameters on noise levels and performance characteristics within an optimization framework. Recent studies (Yu *et al.*, 2020; Casalino *et al.*, 2021; da Silva *et al.*, 2022) have addressed the coupling between CFD aerodynamic predictions and analytical noise prediction models.

In the following, we numerically investigate the effects of the turbulent flow field over an isolated propeller and compute far-field noise using an acoustic analogy. Our objective is to develop and validate a simulation model, based on the open-source code OpenFOAM, to predict noise and aerodynamic characteristics of propellers. The $k-\omega$ SST model (Menter, 1994) is chosen to model the turbulent flow field over a two-blade UAV propeller. The results of this study are expected to contribute as input data for semi-analytical noise prediction methods.

2. METHODS

2.1 Geometry and operating conditions

The flow field over a two-blade propeller geometry of diameter $D = 0.24$ m was simulated. The propeller rotational speed is $n = 100$ RPS and the free-stream velocity is zero. Details of the geometry and descriptions of the measurements carried out in the at the Hong Kong University of Science and Technology (HKUST) can be found in Wu *et al.* (2021a), Wu *et al.* (2021b) and Bu *et al.* (2021). Here we only consider an isolated propeller configuration. In order to improve the quality of the computational mesh, the original geometry was slightly modified by rounding the blade-hub interface and chamfering the tip of the blade. Experimental data for thrust (c_t) and torque (c_q) coefficients, as well as sound pressure level (SPL) measurements are used for validation.

2.2 Numerical model

Unsteady, incompressible Reynolds Averaged Navier-Stokes (URANS) simulations were conducted using the $k-\omega$ SST turbulence model (Menter, 1994) implemented in OpenFOAM v2012 (OpenCFD, 2020). The simulations used a dynamic mesh approach for the rotation of the propeller, in which the domain is divided in a static region and a rotating region. The computational domain and boundary conditions are depicted in Fig. 1. The cylindrical domain has a diameter of $20D$, with the inlet $9D$ upstream and the outlet $11D$ downstream of the propeller.

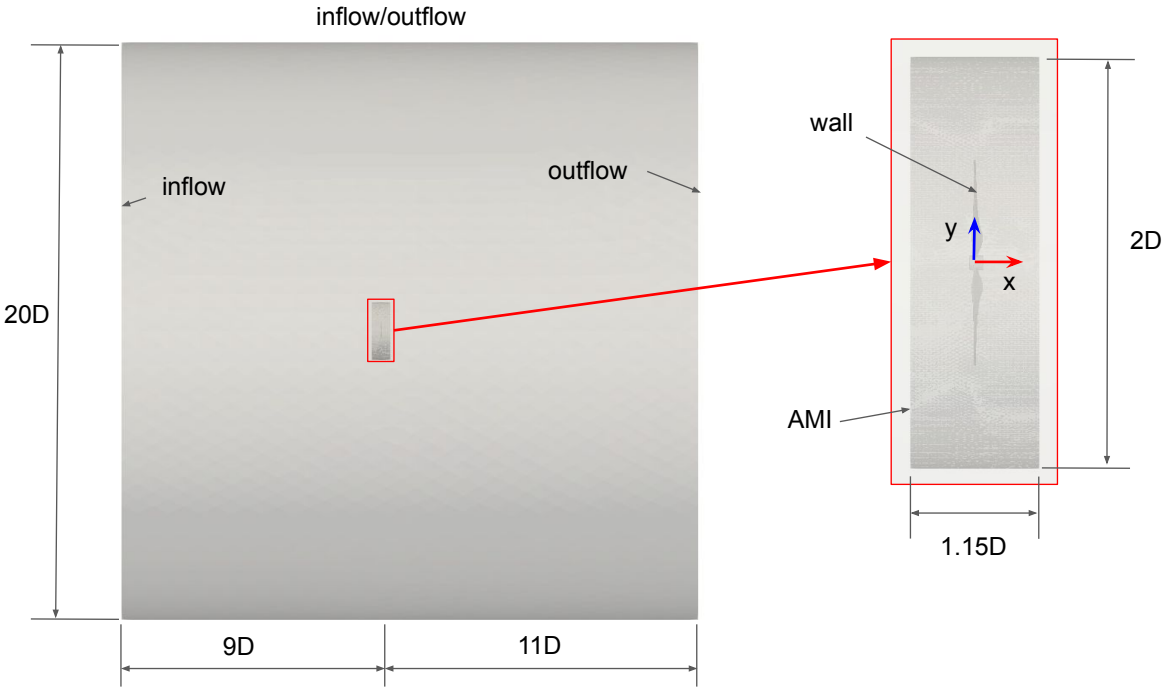

Figure 1: Computational domain and boundary conditions

The simulation was initialized with a small freestream velocity of 1 m/s and a mean gauge-pressure of 0 Pa throughout the domain. A pressure-based inflow condition was imposed at the upstream boundary of the domain while an inflow/outflow condition was used at the lateral boundaries. For computing turbulence quantities, a low turbulence wind tunnel condition was considered, with turbulence intensity $I = 0.1\%$ and $\nu_t/\nu = 5$. For the outflow, a zero-gradient condition was used for velocity and turbulence quantities and an ambient back pressure was imposed. On the propeller surface, a no-slip condition with low-Reynolds wall functions was specified. At the interface between the static and rotating domains, a Cyclic Arbitrary Mesh Interface (AMI) condition was applied. The rotation frequency (n) for the baseline case was 100 RPS.

The computational unstructured grid with 7.62×10^6 volumes, was generated using the open-source software SALOME (SALOME, 2021). The grid is formed predominantly by tetrahedral volumes, as seen in Fig. 2a. Near the walls, layers of prismatic elements were created in order to correctly resolve the boundary layer, shown in Fig. 2b in the near-hub region. The mesh on the surface of the propeller is shown in Figure 2c.

First order numerical were used in the initial timesteps and were switched to second order numerical schemes during the development of the flow. For convective terms, a linear upwind and limited linear schemes were used for velocity and turbulence, respectively, whereas a multi-directional limited linear scheme was used for the gradient terms. For pressure-

velocity coupling, the PIMPLE algorithm was chosen (Holzmann, 2019). The total simulation time is equivalent to 40 complete revolutions with approximately 5000 time-steps per revolution.

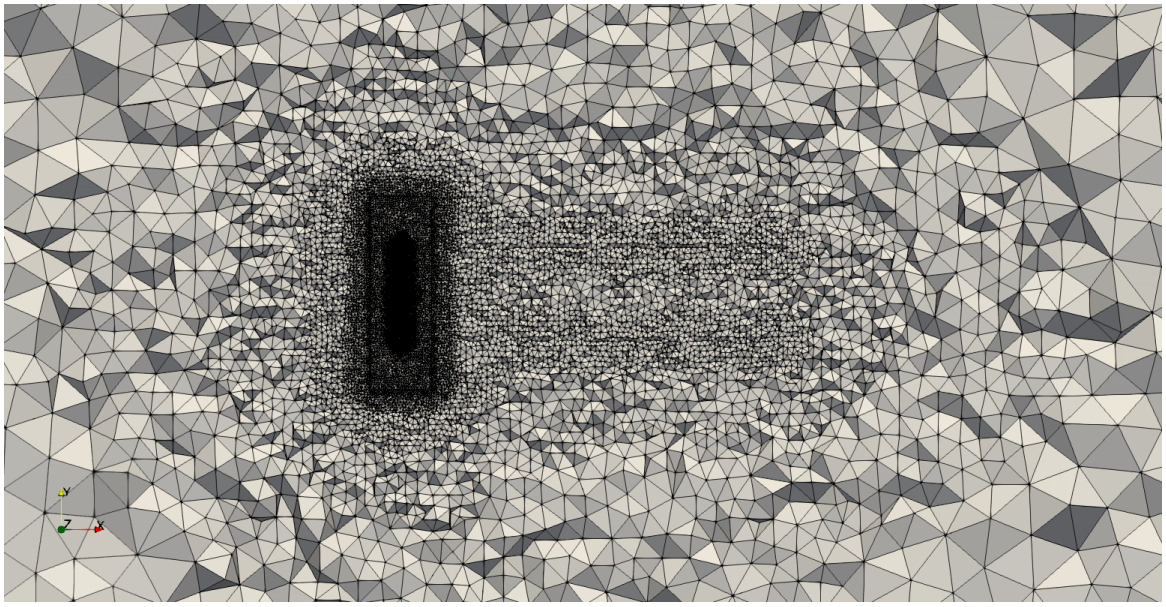

(a) xy plane

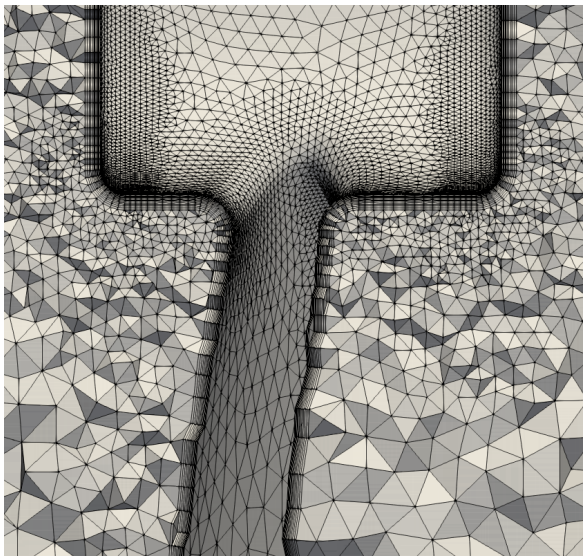

(b) xy plane - near-hub region

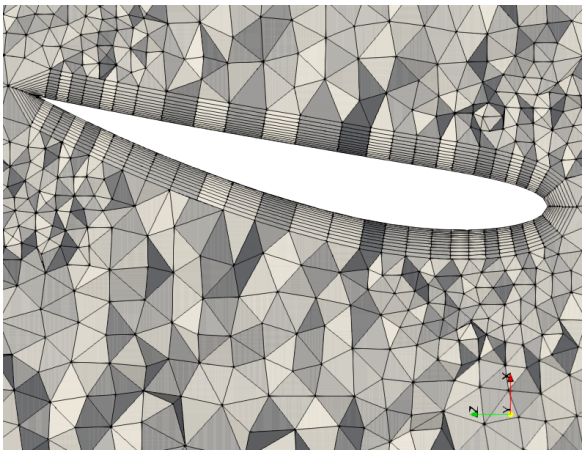

(c) xz plane - y=0.4D

Figure 2: Different slices of the computational domain, showing the computational mesh in different regions.

2.3 Noise computation

Far-field noise computations were calculated by the open-source library libAcoustics, which is integrated with OpenFOAM (Epikhin *et al.*, 2015; llya Evdokimov *et al.*, 2020). This code contains acoustic analogies to be used in conjunction with CFD computations. Validations of the library have been previously reported in the literature (Epikhin *et al.*, 2015; Epikhin, 2021; Chadlvski and da Silva, 2021; Salehian and Mankbadi, 2020).

The Ffwocs-Willians and Hawkings (FWH) analogy based on permeable surfaces was used to compute the far-field noise (Ffowcs Williams and Hawkings, 1969). In this approach, near field pressure and velocity data are stored on an arbitrary control surface, which should encompass the most significant sound-generating regions. This surface information is used as an input for the far-field noise computations. In this study, the Garrick Triangle (GT) formulation (Brès *et al.*, 2010) was used.

Figure 3 shows the permeable surfaces used to collect near-field data in both cases. The surfaces have a cylindrical shape, aligned with the streamwise direction, whose dimensions are shown in the same figure. Surfaces S1, S2 and S3 have the same dimensions except for the streamwise length. Surface S4 has the same streamwise extent as S2, but with

increased diameter. In order to analyze possible effects of spurious noise generated by structures crossing the downstream face of the FW-H surfaces, the downstream face was removed from some computations. The results from these surfaces, labeled as open surfaces, are compared with results from the original, closed surfaces.

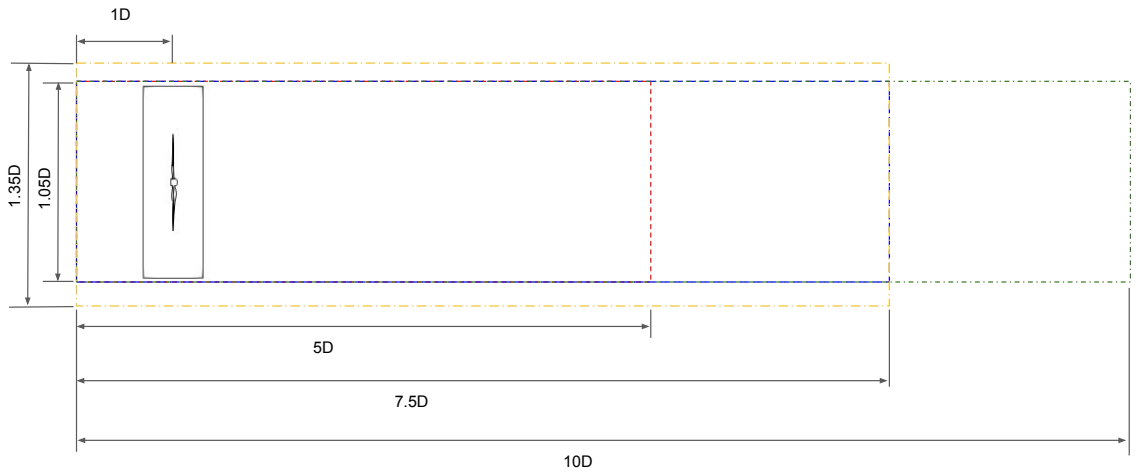

Figure 3: Position of the FWH surfaces. Red - S1, Blue - S2, Green - S3 and Yellow - S4.

The acoustic data were recorded during 21 revolutions, at ten microphone positions shown in Fig. 4, with 1000 timesteps per revolution. The sampling frequency, given by the reciprocal of the timestep, was 100 kHz. The noise power spectral density (PSD) spectrum was obtained using the fast Fourier transform (FFT) algorithm, with resulting frequency resolution of 10 Hz. A Hanning window was employed with an overlap of 75% between blocks.

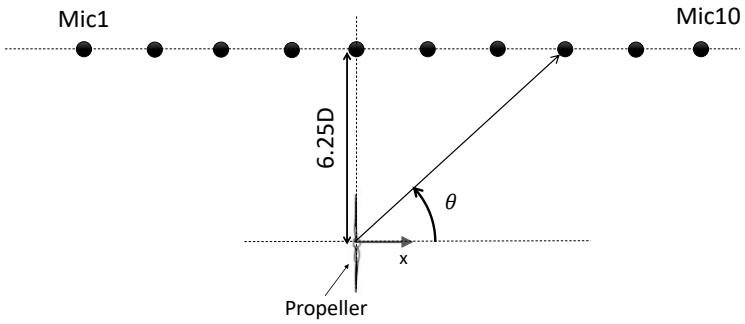

Figure 4: Position of the microphones.

3. RESULTS

3.1 Effect of the FWH surface position

Figure 5 depicts the comparison between the SPL spectra computed from surfaces 1, 2 and 3, in open and closed configurations. As can be seen in Fig. 5a, only slight differences in SPL can be observed at the Blade Passing Frequency (BPF) i.e., 200 Hz. At the second harmonic (400 Hz), Surfaces 1 and 2 show practically the same level, while for Surface 3, the peak level was about 0.8 dB lower.

Results from the open and closed versions of each surface are shown in Figs. 5b-5d. Small differences can be noted for Surface 1, while the spectra are virtually the same for Surfaces 2 and 3. These results indicate that the occurrence of spurious noise owing to the wake crossing of the downstream disk is negligible.

Figure 6 shows the computed SPL for the BPF at each microphone position. By looking at Fig. 6a we can observe deviations of less than 0.5 dB between surfaces. The same observation is true for the comparisons between open and closed surfaces. Regarding surfaces 2 and 4, the differences between the tonal levels were also less than 0.5 dB and the results are omitted for brevity.

From the above we may conclude that very low sensitivity was shown to the length of the FWH surface. Indeed, as URANS simulation do not resolve any turbulent scales, noise sources in the simulation are mainly due the rotating motion of the blades, while the wake noise is negligible. In this sense, truncating the wake may not lead to significant spurious sources. Also, the wake flow did not reach the the end of surface 3 during the simulation time. The closed version of surface 2 is considered for the following analyses.

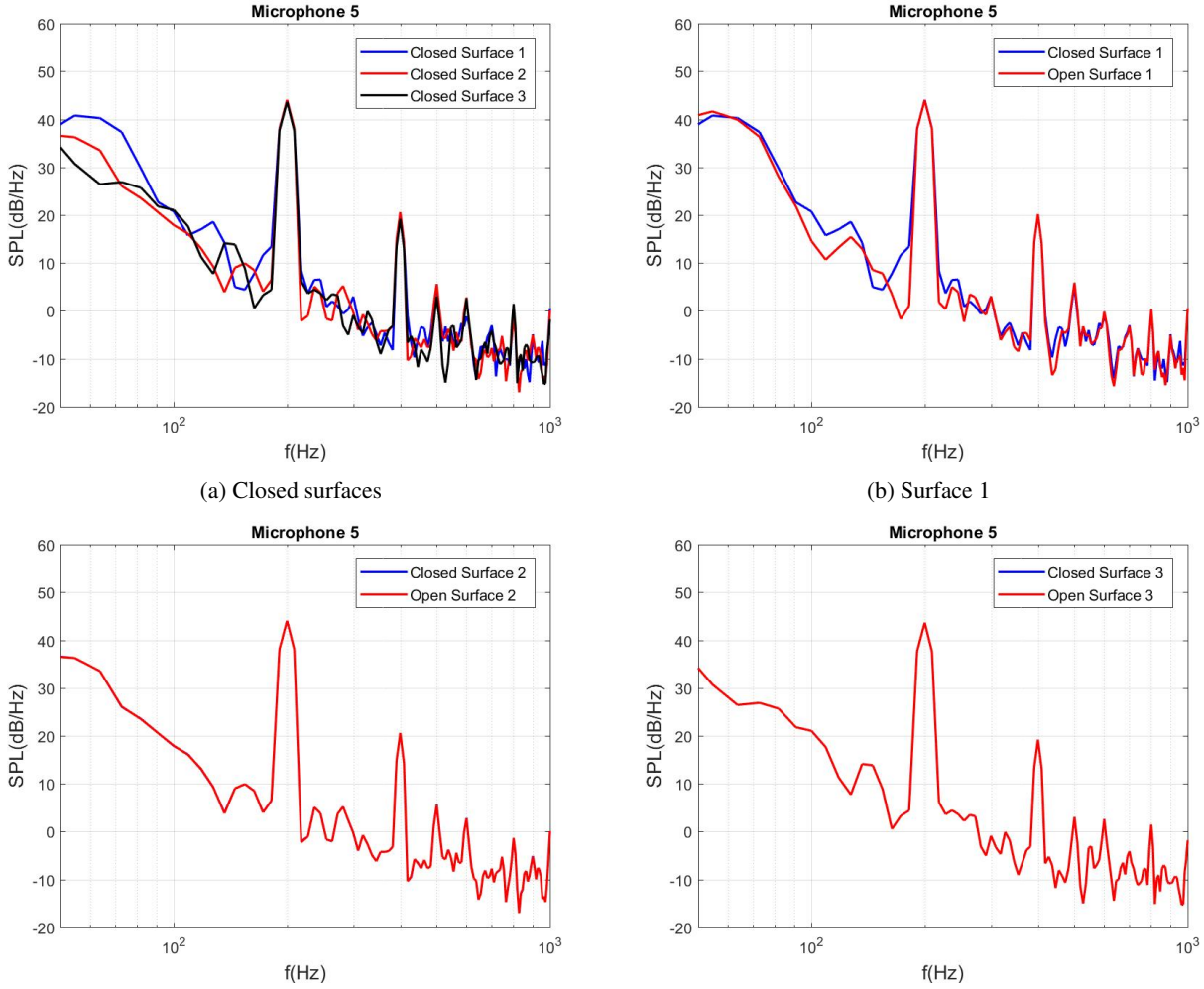

(a) Closed surfaces

(b) Surface 1

(c) Surface 2

(d) Surface 3

Figure 5: Comparison of the SPL spectra obtained from different open and closed FWH Surfaces, for microphone 5, $\theta = 90°$

3.2 Comparisons to experimental data

Table 1 show the comparison between the numerical and experimental aerodynamic coefficients. Numerical results show deviations of about 4.25% and 10.5% for thrust and torque coefficients, respectively. These results are acceptable, considering the limitations of URANS simulations. Future work on grid refinement is expected to improve the accuracy of the predictions.

Table 1: Comparison of aerodynamic coefficients of thrust and torque

	Numerical	Experimental
c_t	0.0675	0.0705
c_q	0.0043	0.0048

The results for PSD spectra of the sound pressure at the observer angle of $\theta = 90°$ are presented in Fig.7(a). Since turbulent scales are not directly resolved in the wake and boundary layers, a correct prediction of the broadband part of the spectra is not expected. On the other hand, for the tonal noise, results are in reasonable agreement with the experiments. The SPL at the BPF was underpredicted by about 2 dB. Regarding the second harmonic, the peak was underpredicted by about 5.5 dB.

Figure 7(b) show the comparison between directivity patterns at the BPF. Predictions underestimated the experimental levels for all the microphone positions. Mean, maximum and minimum deviations were of 2.3, 4.3 and 1 dB, respectively.

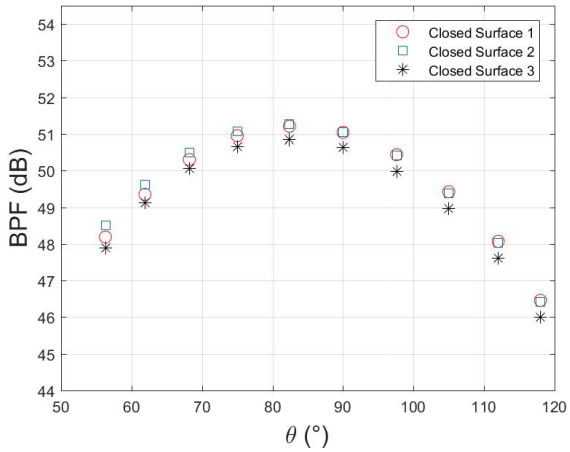

(a) Closed surfaces

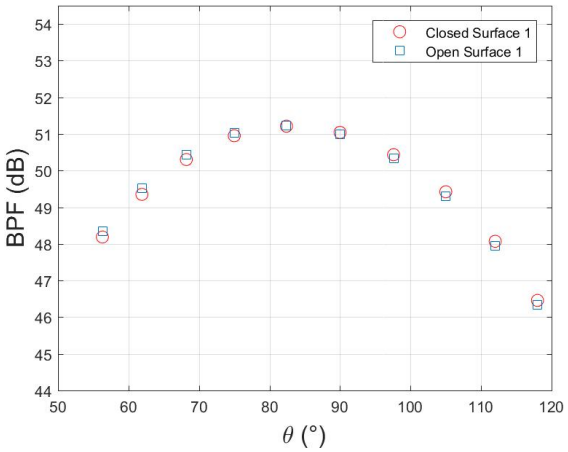

(b) Surface 1

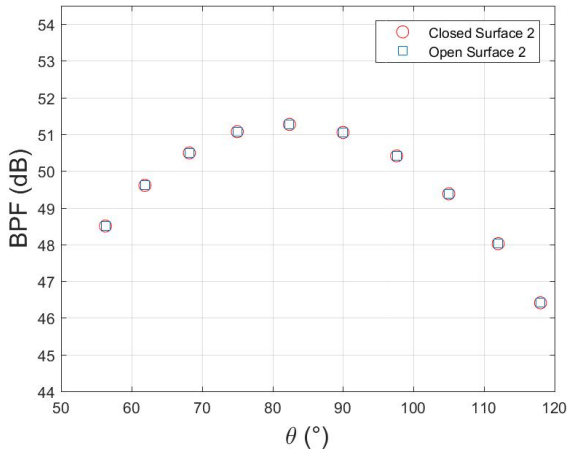

(c) Surface 2

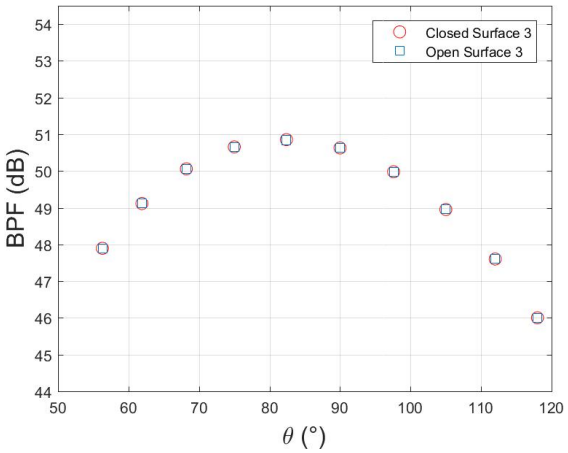

(d) Surface 3

Figure 6: Comparison between the SPL at the blade passing frequency obtained from different FWH surfaces.

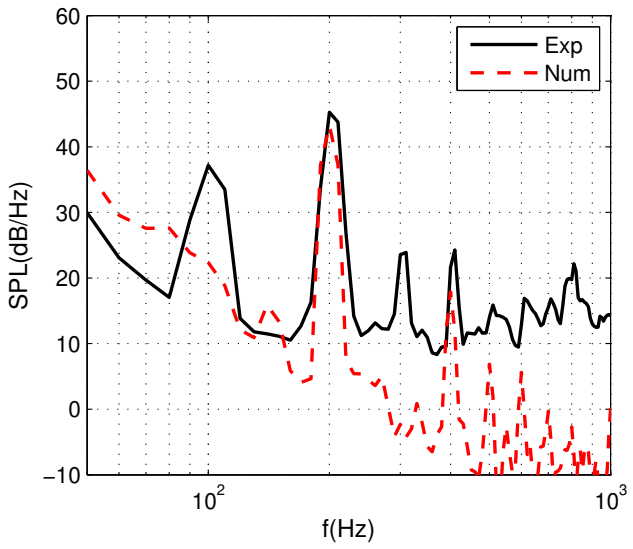

(a) Spectra at $\theta = 90°$.

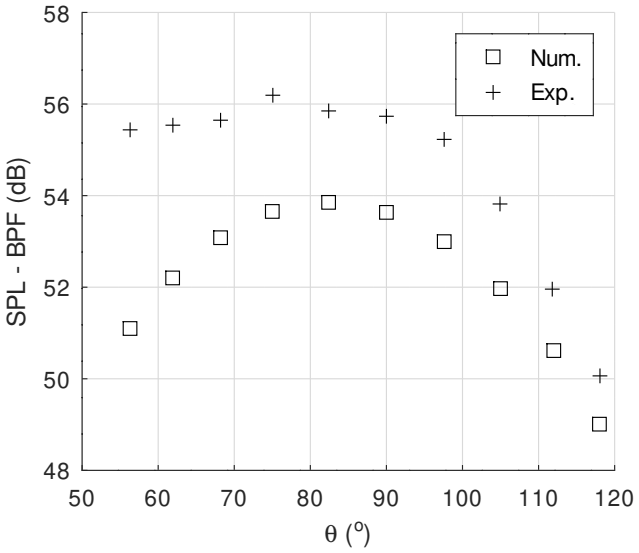

(b) SPL at the BPF

Figure 7: Acoustic field results compared to the experimental data.

4. CONCLUSIONS

We presented and validated a simulation model to predict noise and aerodynamic characteristics of propellers using open-source tools. In general, aerodynamic and acoustics results are in reasonable agreement with experimental data. Acoustic results did not show significant sensitivity to the size of the FWH surfaces and compared favorably with experimental data for the tonal noise level at the blade passing frequency.

Future work will be directed to improve the simulation model by performing sensitivity tests to grid refinement. The aerodynamic data extracted from the simulation will also serve as input to semi-analytical methods to predict tonal and broadband noise.

5. ACKNOWLEDGEMENTS

The authors would like to acknowledge LabCC (Laboratório de Computação Científica) of Universidade Federal de Santa Catarina and the National Laboratory for Scientific Computing (LNCC/MCTI, Brazil) for providing HPC resources, which have contributed to the research results reported within this paper (`http://sdumont.lncc.br`). The authors acknowledge financial support from the National Council for Scientific and Technological Development – CNPq, through call CNPQ/Finep/MCTIC/BRICS-STI No 03/2019, grant 402905/2019-9. The authors also acknowledge Siyang Zhong, from HKUST, for sharing the geometry and experimental data.

6. REFERENCES

Afari, S., Mankbadi, R.R. and Golubev, V.V., 2019. "Towards High-fidelity Analysis of Noise Radiation and Control of Propeller-driven UAV". In *25th AIAA/CEAS Aeroacoustics Conference*. American Institute of Aeronautics and Astronautics, Delft, The Netherlands. ISBN 978-1-62410-588-3. doi:10.2514/6.2019-2632.

Arnhem, N.v., Sinnige, T., Stokkermans, T.C., Eitelberg, G. and Veldhuis, L.L., 2018. "Aerodynamic Interaction Effects of Tip-Mounted Propellers Installed on the Horizontal Tailplane". In *2018 AIAA Aerospace Sciences Meeting*. American Institute of Aeronautics and Astronautics, Kissimmee, Florida. ISBN 978-1-62410-524-1. doi:10.2514/6.2018-2052.

Avallone, F., Casalino, D. and Ragni, D., 2018. "Impingement of a propeller-slipstream on a leading edge with a flow-permeable insert: A computational aeroacoustic study". *International Journal of Aeroacoustics*, Vol. 17, No. 6-8, pp. 687–711. ISSN 1475-472X, 2048-4003. doi:10.1177/1475472X18788961.

Ben Nasr, N., Falissard, F., Decours, J., Gaveriaux, R., Delrieux, Y., Canard-Caruana, S., Laban, M., Brouwer, H., Albreicht, M., Scholz, C., Diette, C. and Chartrain, D., 2017. "Propeller Analysis Using Low & High Fidelity Aero-acoustic Methods". In *35th AIAA Applied Aerodynamics Conference*. American Institute of Aeronautics and Astronautics, Denver, Colorado. ISBN 978-1-62410-501-2. doi:10.2514/6.2017-3573.

Bento, H.F., de Vries, R. and Veldhuis, L.L., 2020. "Aerodynamic Performance and Interaction Effects of Circular and Square Ducted Propellers". In *AIAA Scitech 2020 Forum*. American Institute of Aeronautics and Astronautics, Orlando, FL. ISBN 978-1-62410-595-1. doi:10.2514/6.2020-1029.

Brès, G.A., Pérot, F. and Freed, D., 2010. "A Ffowcs Williams-Hawkings solver for lattice-Boltzmann based computational aeroacoustics". In *Proceedings of the 16th AIAA/CEAS Aeroacoustics Conference - AIAA 2010*. Stockholm.

Bu, H., Wu, H., Bertin, C., Fang, Y. and Zhong, S., 2021. "Aerodynamic and acoustic measurements of dual small-scale propellers". *Journal of Sound and Vibration*, Vol. 511, p. 116330. ISSN 0022-460X. doi:https://doi.org/10.1016/j.jsv.2021.116330.

Casalino, D., Grande, E., Romani, G., Ragni, D. and Avallone, F., 2021. "Definition of a benchmark for low reynolds number propeller aeroacoustics". *Aerospace Science and Technology*, Vol. 113, p. 106707. ISSN 1270-9638. doi:https://doi.org/10.1016/j.ast.2021.106707.

Chadlvski, J.V.V.M. and da Silva, F.D., 2021. "Prediction of aerodynamic noise generated by cylinders in uniform flow using openfoaml aeroacoustics". In *Proceedings of the 26th International Congress of Mechanical Engineering*. doi:10.26678/ABCM.COBEM2021.COB2021-1128.

Chirico, G., Barakos, G.N., Barakos, G., Bown, N. and Bown, N., 2017. "Computational aeroacoustic analysis of propeller installation effects". p. 18.

da Silva, F.D., Batista, P.A., Xavier, G.H. and Chadlvski, J.V.V.M., 2022. "Prediction of the flow and acoustic fields generated by an isolated propeller". In *Proceedings of the 12th Ibero-American Acoustics Congress*. Florianópolis.

Epikhin, A., Evdokimov, I., Kraposhin, M., Kalugin, M. and Strijhak, S., 2015. "Development of a dynamic library for computational aeroacoustics applications using the openfoam open source package". *Procedia Computer Science*, Vol. 66, pp. 150–157.

Epikhin, A., 2021. "Validation of the developed open source library for far-field noise prediction". In *Proceedings of the 27th International Congress on Sound and Vibration*. Silesian University Press, Denver, Colorado. ISBN 9788378807995.

Ffowcs Williams, J.E. and Hawkings, D.L., 1969. "Sound generated by turbulence and surfaces in arbitrary motion".

Philosophical Transactions of the Royal Society, Vol. A264, No. 1151, pp. 321–342.

Hambrey, J., 2017. *Computational Aeroacoustic Prediction of Propeller Noise Using Grid-Based and Grid-Free CFD Methods*. Master of Applied Science, Carleton University, Ottawa, Ontario. doi:10.22215/etd/2017-11724.

Holzmann, T., 2019. *Mathematics, Numerics, Derivations and OpenFOAM®*.

llya Evdokimov, UniCFD and Epikhin, A., 2020. "unicfdlab/libacoustics: Openfoam+ v1912 version of libacoustics". doi:10.5281/zenodo.3878439.

Menter, F.R., 1994. "Two-equation eddy-viscosity turbulence models for engineering applications". *AIAA Journal*, Vol. 32, No. 8, pp. 1598–1605. doi:10.2514/3.12149. _eprint: https://doi.org/10.2514/3.12149.

OpenCFD, 2020. "Openfoam: the open source cfd toolbox user guide". OpenCFD Ltd, https://www.openfoam.com/documentation/overview. Accessed 17 June 2021.

Salehian, S. and Mankbadi, R., 2020. "Jet noise in airframe integration and shielding". *Applied Sciences*, Vol. 10, No. 2. ISSN 2076-3417. doi:10.3390/app10020511.

SALOME, 2021. "Salome v9.8 user guide". docs.salome-platform.org/latest/main/index.html Accessed 20 June 2022.

Stokkermans, T.C., Nootebos, S. and Veldhuis, L.L., 2019. "Analysis and Design of a Small-Scale Wingtip-Mounted Pusher Propeller". In *AIAA Aviation 2019 Forum*. American Institute of Aeronautics and Astronautics, Dallas, Texas. ISBN 978-1-62410-589-0. doi:10.2514/6.2019-3693.

Wu, H., Zheng, C., Zhou, P., Fattah, R., Zhong, S. and Zhang, X., 2021a. "The multi-functional rotor aerodynamic and aeroacoustic test platform at hkust". doi:10.3397/IN-2021-2695.

Wu, H., Zhou, P., Zhong, S., Zhang, X., Li, Q. and Luo, K., 2021b. "Experimental assessment of the noise characteristics of propellers for commercial drones". doi:10.3397/IN-2021-2697.

Yu, P., Peng, J., Bai, J., Han, X. and Song, X., 2020. "Aeroacoustic and aerodynamic optimization of propeller blades". *Chinese Journal of Aeronautics*, Vol. 33, No. 3, pp. 826–839. ISSN 1000-9361. doi:https://doi.org/10.1016/j.cja.2019.11.005.

7. RESPONSIBILITY NOTICE

The authors are solely responsible for the printed material included in this paper.